APPLIED AND ENVIRONMENTAL MICROBIOLOGY, Aug. 2003, p. 4901–4909 Vol. 69, No. 8
0099-2240/03/$08.00+0 DOI: 10.1128/AEM.69.8.4901–4909.2003

Strain-Specific Ureolytic Microbial Calcium Carbonate Precipitation

Frederik Hammes,[1]† Nico Boon,[1] Johan de Villiers,[2] Willy Verstraete,[1]* and Steven Douglas Siciliano[1]‡

Laboratory of Microbial Ecology and Technology (LabMET), Ghent University, B-9000 Ghent, Belgium,[1] and Department of Earth Sciences, University of Pretoria, 0001 Pretoria, South Africa[2]

Received 5 December 2002/Accepted 2 May 2003

During a study of ureolytic microbial calcium carbonate ($CaCO_3$) precipitation by bacterial isolates collected from different environmental samples, morphological differences were observed in the large $CaCO_3$ crystal aggregates precipitated within bacterial colonies grown on agar. Based on these differences, 12 isolates were selected for further study. We hypothesized that the striking differences in crystal morphology were the result of different microbial species or, alternatively, differences in the functional attributes of the isolates selected. Sequencing of 16S rRNA genes showed that all of the isolates were phylogenetically closely related to the *Bacillus sphaericus* group. Urease gene diversity among the isolates was examined by using a novel application of PCR-denaturing gradient gel electrophoresis (DGGE). This approach revealed significant differences between the isolates. Moreover, for several isolates, multiple bands appeared on the DGGE gels, suggesting the apparent presence of different urease genes in these isolates. The substrate affinities (K_m) and maximum hydrolysis rates (V_{max}) of crude enzyme extracts differed considerably for the different strains. For certain isolates, the urease activity increased up to 10-fold in the presence of 30 mM calcium, and apparently this contributed to the characteristic crystal formation by these isolates. We show that strain-specific calcification occurred during ureolytic microbial carbonate precipitation. The specificity was mainly due to differences in urease expression and the response to calcium.

Numerous diverse microbial species participate in the precipitation of mineral carbonates in various natural environments, including soils, geological formations, freshwater biofilms, oceans, and saline lakes (9, 28, 30, 31). In some instances the resulting natural precipitates represent the fossil records or fingerprints of bacterial activity (28, 38, 40). For example, this process was at the heart of the original debate about whether mineral sediments on the ALH84001 Martian meteorite represent proof of life in outer space (24, 39, 40). In addition to its natural historical importance, microbial carbonate precipitation (MCP) is also the basis of several innovative applications in both the building sector and the wastewater industry (13, 15, 16, 37).

The precise role of microbes in the carbonate precipitation process is still not clear. Boquet et al. (5) suggested that almost all bacteria are capable of $CaCO_3$ precipitation. Knorre and Krumbein (20) concluded that MCP occurs as a by-product of common microbial metabolic processes, such as photosynthesis, urea hydrolysis, and sulfate reduction. These metabolic processes increase the alkalinity (increase the pH and dissolved inorganic carbon content) of the environment and thereby favor $CaCO_3$ precipitation (8, 9). Alternatively, it is possible that there are specific attributes of certain bacteria that promote and affect $CaCO_3$ precipitation. The negatively charged nature and specific functional groups of microbial cell walls favor the binding of divalent cations (Ca^{2+}, Mg^{2+}), thereby making microorganisms ideal crystal nucleation sites (30, 34). Microbial extracellular polymeric substances are also an important factor in precipitation, either through trapping and concentration of calcium ions or as a result of specific proteins that influence precipitation (19). Kawaguchi and Decho (19) suggested that specific proteins present in biological extracellular polymeric substances cause the formation of different $CaCO_3$ polymorphs. A third hypothesis combines the common metabolism and strain specificity hypotheses to suggest that $CaCO_3$ precipitation, possibly influenced by intracellular calcium metabolism (8, 17, 23), might play a role in the ecology of the precipitating organism (2, 23).

Enzymatic hydrolysis of urea presents a straightforward model for studying microbial $CaCO_3$ precipitation. The urease enzyme (urea amidohydrolase; EC 3.5.1.5) is common in a wide variety of microorganisms, can be readily induced by adding an inexpensive substrate, and is involved in several biotechnological applications (12, 16, 37). One mole of urea is hydrolyzed intracellularly to 1 mol of ammonia and 1 mol of carbamate (equation 1), which spontaneously hydrolyzes to form an additional 1 mol of ammonia and carbonic acid (equation 2) (7). These products subsequently equilibrate in water to form bicarbonate and 2 mol of ammonium and hydroxide ions (equations 3 and 4). The latter give rise to a pH increase, which in turn can shift the bicarbonate equilibrium, resulting in the formation of carbonate ions (equation 5), which in the presence of soluble calcium ions precipitate as $CaCO_3$ (equation 6) (7, 8).

$$CO(NH_2)_2 + H_2O \rightarrow NH_2COOH + NH_3 \quad (1)$$

$$NH_2COOH + H_2O \rightarrow NH_3 + H_2CO_3 \quad (2)$$

* Corresponding author. Mailing address: Laboratory of Microbial Ecology and Technology (LabMET), Ghent University, Coupure Links 653, B-9000 Ghent, Belgium. Phone: 32-(0)9 264 59 76. Fax: 32-(0)9 264 62 48. E-mail: Willy.Verstraete@rug.ac.be.

† Present address: Department of Microbiology and Molecular Ecotoxicology, Swiss Federal Institute for Environmental Science and Technology, CH-8600 Duebendorf, Switzerland.

‡ Present address: Department of Soil Science, University of Saskatchewan, Saskatoon, Saskatchewan S7N 5A8, Canada.

$$H_2CO_3 \leftrightarrow HCO_3^- + H^+ \ (pK_{a2} = 6.37) \quad (3)$$

$$2NH_3 + 2H_2O \leftrightarrow 2NH_4^+ + 2OH^- \quad (4)$$

$$HCO_3^- + H^+ + 2NH_4^+ + 2OH^- \leftrightarrow CO_3^{2-} + 2NH_4^+ + 2H_2O \quad (5)$$

$$CO_3^{2-} + Ca^{2+} \leftrightarrow CaCO_3 \ (K_{so} = 3.8 \times 10^{-9}) \quad (6)$$

During laboratory work over the past few years, we found that different bacterial isolates precipitated visually different crystal aggregates in a repeatable manner when they were cultivated on semisolid media under similar growth conditions. The aim of this work was to characterize some of the primary mechanisms responsible for this diversity in crystal aggregate morphology.

MATERIALS AND METHODS

Isolation. $CaCO_3$-precipitating strains were isolated from two soils (garden soil and landfill soil from Ghent, Belgium), from a freshly cut concrete surface (Portland, type CEM I 42.5 R), and from calcareous sludge from a biocatalytic calcification reactor. The latter treats calcium-rich industrial wastewater through ureolytic microbial carbonate precipitation (15, 16). The natural samples were suspended in a sterile physiological solution (8.5 g of NaCl liter^{-1}), diluted appropriately, and plated on precipitation agar containing (per liter) 3 g of nutrient broth (Oxoid), 20 g of urea (Riedel-de Haën), 2.12 g of $NaHCO_3$ (Sigma), 10 g of NH_4Cl (Sigma), and 30 mM $CaCl_2 \cdot 2H_2O$ (Sigma) (12, 37). Incubation was at 28°C. Colonies were assessed every 5 days with a stereomicroscope (Wild, Heerbrugg, Belgium), and positive colonies were selected based on visual crystal formation within 10 days. Positive isolates were purified by repetitive dilution and plating (as described above). The purified strains were deposited in the BCCM/LMG Culture Collection (Ghent, Belgium) as strains LMG21776 to LMG21787.

Microscopy and phase identification. Crystal-precipitating colonies were examined after 5 and 10 days of cultivation by light microscopy with an Axioskop II Plus microscope (Zeiss) and by stereomicroscopy (Wild). Digital images were captured with a 1-CCD camera (Hamamatsu Photonics GmbH, Herssching, Germany). A total of 12 isolates were selected based on visual differences in precipitate morphology. Large crystal aggregates that precipitated within single colonies of the isolates were subsequently harvested from the agar surface, washed in sterile water, and dried (28°C, 3 days). The dried aggregates were ground to the appropriate particle size for X-ray diffraction (XRD) analysis (diameter, <10 μm) with a McCrone micronizing mill and then analyzed by using a Siemens D-501 diffractometer equipped with an Ni filter and a CuKα radiation source. Phase identification was done after background subtraction by using the Bruker EVA software.

Urease activity and location of urease activity. All the isolates were tested for urease activity, as well as the location of urease activity. This was done by streaking the purified cultures on urease test agar (BBL, Becton Dickinson and Company, Sparks, Md.) and inoculating urease test broth (as described above) with viable liquid cultures, as well as filtrates (pore size, 0.22 μm; Millipore) of the liquid cultures. A change in color following incubation for 5 days at 28°C was recorded as a urease-positive reaction.

PCR amplification of 16S rRNA genes. A DNA template for PCR amplification from pure cultures was obtained by extracting total genomic DNA according to the manufacturer's instructions (Wizard genomic DNA purification kit; Promega, Leiden, The Netherlands). The PCR master mixture contained each primer at a concentration of 500 nM, each deoxynucleoside triphosphate at a concentration of 200 μM, 1.5 mM $MgCl_2$, 10 μl of thermophilic DNA polymerase 10× reaction buffer ($MgCl_2$ free), 2.5 U of *Taq* DNA polymerase (Promega, Madison, Wis.), 400 ng of bovine serum albumin (Boehringer) per μl, and enough DNase- and RNase-free filter-sterilized water (Sigma-Aldrich Chemie, Steinheim, Germany) so that the final volume was 100 μl. One microliter of DNA template was added to 24 μl of the master mixture. The 16S rRNA gene fragments were obtained by amplifying the 16S rRNA gene with primers P63f (5′-CAGGCCTAACACATGCAAGTC-3′) and P1378r (5′-CGGTGTGTACAAGGCCCGGGAACG-3′). PCR was performed in a 9600 thermal cycler (Perkin-Elmer, Norwalk, Conn.) with a program consisting of 10 min at 95°C, followed by 30 cycles of 1 min at 94°C, 1 min at 53°C, and 2 min at 72°C and a final elongation step for 10 min at 72°C.

PCR-DGGE of the *ureC* gene. For PCR-denaturing gradient gel electrophoresis (DGGE) analysis of the *ureC* gene the DNA extraction procedure and the PCR master mixture composition were identical to those described above. *Bacillus pasteurii* ATCC 6453 was included as a positive control for ureolytic microbial $CaCO_3$ precipitation (12, 37). To amplify the genes coding for the *ureC* subunit of the urease enzyme, PCR was performed with primers UreC-F (5′-TGGGCCTTAAAATHCAYGARGAYTGGG-3′) and UreC-R (5′-GGTGGTGGCACACCATNANCATRTC-3′) as previously described by Reed (29). The length of the expected amplified fragment was 382 bp. To examine the diversity of the partial *ureC* DNA fragments by DGGE, a 40-bp GC clamp (5′-CGCCCGCCGCGCGGCGGGCGGGGCGGGGGCACGGGGGG-3′) (27) was attached to the 5′ end of the UreC-F primer. The PCR conditions were as follows: 94°C for 5 min, followed by 35 cycles of 92°C for 1 min, 50°C for 1 min, and 72°C for 2 min. A final extension was carried out at 72°C for 10 min. DGGE was performed with the Bio-Rad D gene system (Bio-Rad, Hercules, Calif.). PCR samples were loaded onto 7% (wt/vol) polyacrylamide gels in 1× TAE (20 mM Tris, 10 mM acetate, 0.5 mM EDTA; pH 7.4). The polyacrylamide gels were made with a 40 to 60% denaturing agent gradient; 7 M urea and 40% formamide were defined as 100% denaturing agent. Electrophoresis was performed for 16 h at 60°C and 45 V. The resulting gels were stained with SYBR Green I nucleic acid gel stain (1:10,000 dilution; FMC BioProducts, Rockland, Maine) and photographed (3). Processing of the DGGE gels was done with the Bionumerics 2.0 software (Applied Maths, Kortrijk, Belgium). Calculation of similarities was based on the Dice correlation coefficient and the results in a distance matrix. The unweighted pair group with mathematical average clustering algorithm was used to calculate dendrograms for the DGGE gels.

DNA sequencing and sequence analysis. DNA sequencing of the PCR fragments was carried out by ITT Biotech-Bioservice (Bielefeld, Germany). Analysis of DNA sequences and homology searches were completed by using standard DNA sequencing programs and the BLAST server of the National Center for Biotechnology Information (www.ncbi.nlm.nih.gov) with the BLAST algorithm (1) and specifically with the blastn program for comparison of a nucleotide query sequence with a nucleotide sequence database. A phylogenetic tree was constructed by using the RDP Phylip 3.5c interface (22). Distance matrix analyses were done with the Jukes-Cantor (18) correction, and tree construction was done by the neighbor-joining method (33). Putative *ureC* gene fragments were excised from a DGGE gel, reamplified, and sent out for sequencing (see above). The resulting nucleotide sequences were translated into protein sequences by using the blastx software (BLAST) (National Center for Biotechnology Information), and these sequences were compared with a protein sequence database.

Protein extraction. Isolates were cultivated in 1 liter of nutrient broth (Oxoid) containing 20 g of urea liter^{-1} for 48 h at 30°C with shaking (100 rpm). Bacterial cells were harvested by centrifugation (8,000 × *g*, 30 min) and washing of the pellet in extraction buffer (100 mM NaH_2PO_4, 1 mM EDTA; pH 7.0), followed by centrifugation (15,000 × *g*, 10 min) and resuspension in extraction buffer (see above). Crude enzyme was extracted by bead beating (three 90-s pulses with 10-s pauses between pulses). The protein concentration was determined by the procedure of Bradford (6). This included adding 200 μl of a commercial Bio-Rad protein assay solution to 800 μl of an appropriately diluted sample and measuring the color development spectrophotometrically at 595 nm. Bovine serum albumin was used as the standard.

Urease activity assay. Urease activity was assayed in 1 ml of buffer containing 100 mM NaH_2PO_4 and 1 mM EDTA (pH 8.0). Ten different substrate (urea) concentrations between 5 and 100 mM were used. Both the crude enzyme and the reaction mixtures were incubated for 5 min at 25°C prior to the urease assay. The reaction was initiated by addition of the crude enzyme, and urease activity was determined by measuring the amount of total ammonium nitrogen released after 10 min spectrophotometrically (425 nm) by using the Nessler assay method (14). One unit of urease activity was defined as the amount of enzyme that hydrolyzed 1 μmol of urea per min. Michaelis-Menten kinetic constants (K_m and V_{max}) were estimated by graphing the data in a Lineweaver-Burk plot. In another assay to determine the effect of pH on the relative urease activity, the procedure described above was repeated with 50 mM urea solutions at pH 7 and 8 (in 100 mM phosphate buffer) and pH 9 (in 100 mM Tris-HCl buffer). In both assays, commercial urease from Jack beans (type III from Jack beans; Sigma) was used as a positive control.

Effect of calcium on urease activity. The isolates were cultivated and concentrated as described above. Sterile solutions containing urea (100 mM), nutrient broth (1 g · liter^{-1}), and $NaHCO_3$ (10 mM) at pH 7 (1 N HNO_3) were prepared and inoculated along with the isolates to obtain final concentrations of 10^7 to 10^8 CFU · ml^{-1}. Similar solutions that also contained 30 mM $CaCl_2$ were also inoculated. These solutions were all incubated at 25°C with stirring and were sampled every 30 min. Total ammonium nitrogen was measured as described above, and

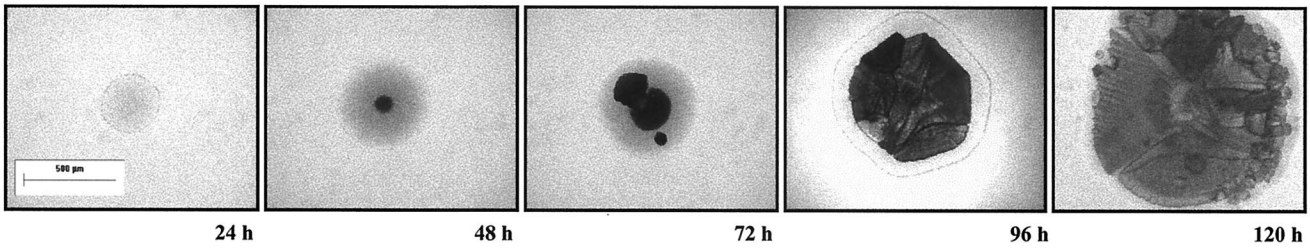

FIG. 1. Typical ureolytic $CaCO_3$ precipitation sequence, starting with the formation of amorphous $CaCO_3$, followed by crystallization and crystal maturation.

the results were expressed as the urease activity in the presence of calcium divided by the urease activity in the absence of calcium. All experiments were done in triplicate, and all measurements were obtained in duplicate.

PCA, multivariate analysis of variance, and discriminant analysis. Principal-component analysis (PCA) was carried out by using Bionumerics software and incorporating as parameters for each isolate (i) the number of urease bands from the DGGE, (ii) the Ca^{2+}/urea ratio, (iii) the K_m data, (iv) the V_{max} data, and (v) the calcium-urease activity data. This was done to establish a statistical correlation between the various parameters and the morphological differences observed in the crystal aggregates. Multivariate analysis of variance and discriminant analysis were also used to identify the parameter(s) that was the primary contributing parameter(s) to these morphological differences. The following three different groups were defined based on the PCA: (i) strains CPB 1 to CPB 4, (ii) strains CPB 5 and CPB 6, and (iii) strains CPB 7 to CPB 12. Accounting for covariance structure and relative character importance were both used in the discriminant calculations.

Nucleotide sequence accession numbers. The almost complete sequences (800 to 1,300 kb) of 16S rRNA genes of all isolates have been deposited in the GenBank database under accession no. AF548874 to AF548885. Six nucleotide sequences (±300 kb) of urease genes have also been deposited in the GenBank database under accession no. AY178982 to AY178987.

RESULTS

Isolation, crystallization, and initial urease analysis. About 10% of all bacterial colonies isolated from various sources induced crystallization on the precipitation agar. Precipitation started with a darkening in the center of the bacterial colony, which was attributed to amorphous $CaCO_3$ formation (after between 20 h and 5 days, depending on the isolate), and this was followed by crystallization and crystal maturation with time (Fig. 1). The precipitate always formed within the bacterial colony on the agar surface, which also captured bacteria within the crystal structure. Twelve isolates were selected for further study based on morphological differences observed in the large crystal aggregates which were precipitated in single colonies on precipitation agar (Fig. 2). The isolates were termed calcium-precipitating bacteria (strains CPB 1 to CPB 12). Four basic morphologically distinct groups of crystal aggregates were initially distinguished. CPB 1 to CPB 4 all produced large, light-brown structures which formed rapidly (20 to 48 h for crystallization), and aggregates accounted for up to 98% of the total colony surface (Fig. 2). CPB 5 and CPB 6 precipitated at similar rates, but in this case the result was distinctly sharp, whitish and transparent crystal aggregates. CPB 7 to CPB 10 precipitated at noticeably lower rates than the first strains (about 3 to 5 days for crystallization). The resulting precipitates were thick, brown aggregates, with an almost sponge-like appearance. CPB 11 and CPB 12 required between 5 and 10 days for crystallization and were characterized by initial formation of separate, small, spherical crystals that coalesced only after a couple of days. Note that the different crystal groups reflected neither the initial origin of the isolates (indicated in Fig. 2) nor the cell morphology, since all isolates formed rod-shaped cells that were between 1 and 3 μm long. XRD analysis of the crystals revealed that the primary crystal component of all the classes was rhombohedral calcite, although hexagonal vaterite was detected in some cases as well. For all isolates, urease activity was cell associated. All 12 isolates produced a urease-positive color when they were grown on urease test agar or when they were inoculated into urease test broth. No filtrate of a liquid culture gave a positive reaction.

Identification and sequencing. All of the isolates were closely related to one another and to cultured bacteria belonging to the *Bacillus sphaericus* group. BLAST results suggested that the closest relatives of this group are *Bacillus pasteurii* (CPB 1 to CPB 4), *Bacillus psychrophilus* (CPB 5 to CPB 7), *Planococcus okeanokoites* (CPB 8), and *Bacillus globisporus* (CPB 9 to CPB 12), while another species that is closely related to all of the isolates is *Filibacter limicola*. A phylogenetic (neighbor-joining) tree was constructed by using *Escherichia coli* and *B. subtilis* as outgroups (Fig. 3). Although all of the CPB isolates were related to the *B. sphaericus* group, there was still sufficient diversity in the 16S rRNA genes to place the isolates into different clusters. The largest cluster contained CPB 1 to CPB 4, CPB 7, and CPB 8 and was closely related to *B. pasteurii*. The second cluster contained CPB 11 and CPB 12, and the third cluster contained CPB 10. CPB 9 was situated between the second and third clusters. The fourth cluster contained CPB 5 and CPB 6 and was noticeably distantly related to the other clusters.

Urease gene diversity. PCR-DGGE, performed with UreC primers, revealed that the positions and numbers of bands were different for different isolates (Fig. 4), and a cluster analysis, based on band positions, showed that there were two large groups, as well as four isolates that were not in any group (CPB 7, CPB 8, CPB 10, and CPB 12). The first group included CPB 1 and CPB 2 (100% similarity), CPB 11, CPB 3, and CPB 4. The second group included CPB 5 and CPB 6 (100% similarity) and CPB 9, as well as *B. pasteurii*. All of the bands were excised from the DGGE gel, but only six bands (as indicated in Fig. 3) were successfully purified, amplified, and sequenced. In all cases, amino acid sequences were related to the alpha subunit (UreC) of previously described ureases, thus indicating that the PCR amplification was indeed specific. The highest levels of similarity were found with sequences from *Bacillus halodurans* (NP_241120.1), *Corynebacterium glutamicum*

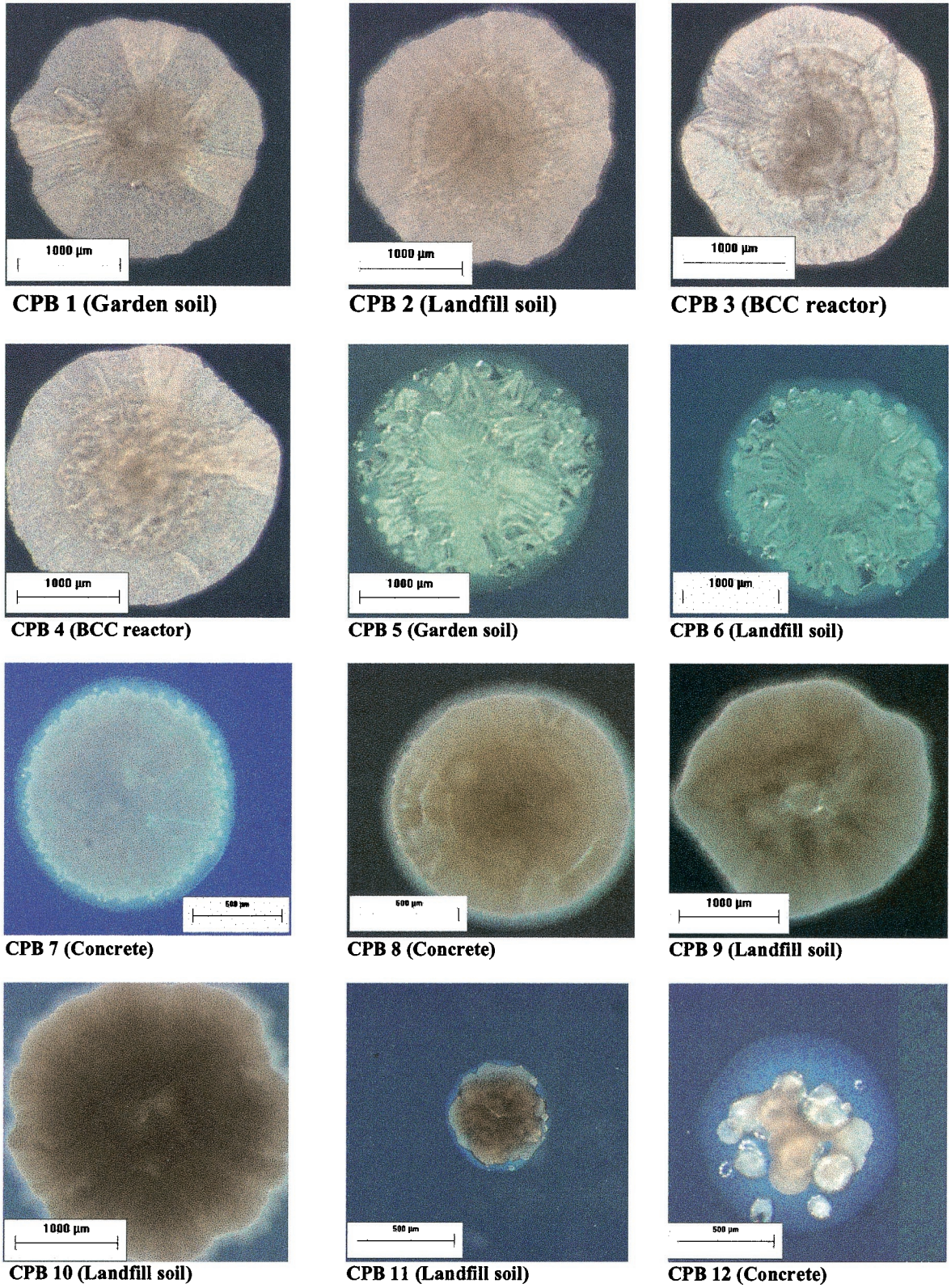

FIG. 2. Morphological differences in calcite precipitates within bacterial colonies of ureolytic calcium-precipitating bacteria grown on semisolid media. The origins of isolates are indicated in parentheses.

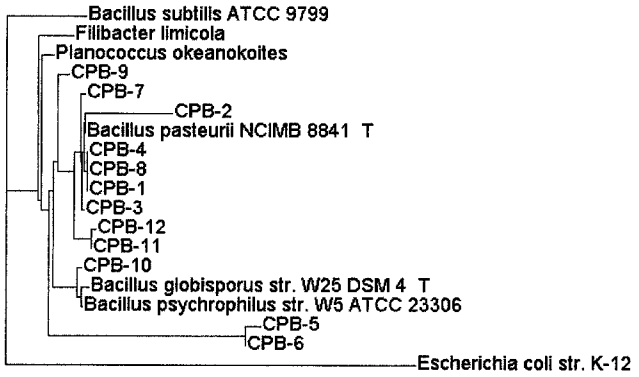

FIG. 3. Neighbor-joining tree, based upon partial 16S rRNA gene sequences of the 12 isolates (CPB 1 to CPB 12) and their closest relatives. *E. coli* was used as an outgroup. A sequence analysis was done as described in the text, and 402 base positions were included in the calculations.

(NP_599339.1), *B. pasteurii* (S_47104), and *Haemophilus influenzae* (NP_438697.1). The levels of similarity between the isolate sequences and these corresponding sequences ranged from 66 to 90%, and the levels of similarity between the isolate sequences ranged from 81 to 95%.

Urease activity. There were some distinct differences among the isolates when both the substrate affinity (K_m) and rate (V_{max}) values were compared (Fig. 5). Isolates CPB 1 to CPB 6 showed high urea affinities, while the affinities of CPB 7 to CPB 12 were about three times lower. Isolates CPB 5 and CPB 6 displayed noticeably high V_{max} values, while the V_{max} values of CPB 7 and CPB 11 were distinctly lower than the other V_{max} values. For all the isolates, the relative activity of the crude enzyme extract was between 40 and 60% lower at pH 7 than at pH 8, while pH 9 had no significant effect at all (results not shown).

Effect of calcium on urease activity. Figure 6 shows a comparison between the urease activities of the isolates with and without calcium added to the medium. CPB 1 to CPB 4 displayed large increases in urease activity (4- to 10-fold) in the presence of calcium ions compared to the activity in the absence of calcium. For the other isolates there were either no differences or calcium had slightly adverse effects on the urease activities.

PCA. PCA confirmed that at least three crystal groups could be explained by the various urease data, thereby suggesting that the differences in precipitation could largely be ascribed to diversity in the urease gene fragments of the isolates, with resulting biochemical differences in the urease activities of the isolates (Fig. 7). The first three principal components (PC) explained 99.7% of the total variation (PC 1, 79.4%; PC 2, 18.9%; PC 3, 1.4%). The PCA, however, did not separate the different crystal aggregate groups completely; most notably, CPB 11 and CPB 12 clustered together with CPB 7 to CPB 10. Based on the PCA, three groups were included in the discriminant analysis. The results showed that for the first discriminant (accounting for 91% of the discrimination) in descending order of importance, the substrate affinity (K_m) made a positive contribution, while the maximum hydrolysis rate (V_{max}) and the number of bands both made negative contributions ($P = 0.008$).

DISCUSSION

The aim of this study was to investigate the primary mechanisms that cause apparent differences in crystal aggregate formation during ureolytic MCP. Such information should be of particular interest to workers investigating carbonate precipitation as a bacterial fossil record and to workers investigating carbonate precipitation as a potential biotechnological technique. MCP is an established tool for the in situ restoration of buildings and monuments (8, 37) and is an emerging tool in the treatment of calcium-rich industrial wastewater (15, 16). For both these applications, improved knowledge of the precise role of bacteria in the precipitation process, specifically the mechanisms governing precipitation rates and types, is vitally important (8). For example, recent biotechnology designed to remove Ca^{2+} from industrial wastewater specifically stimulates and accelerates urease activity in activated sludge,

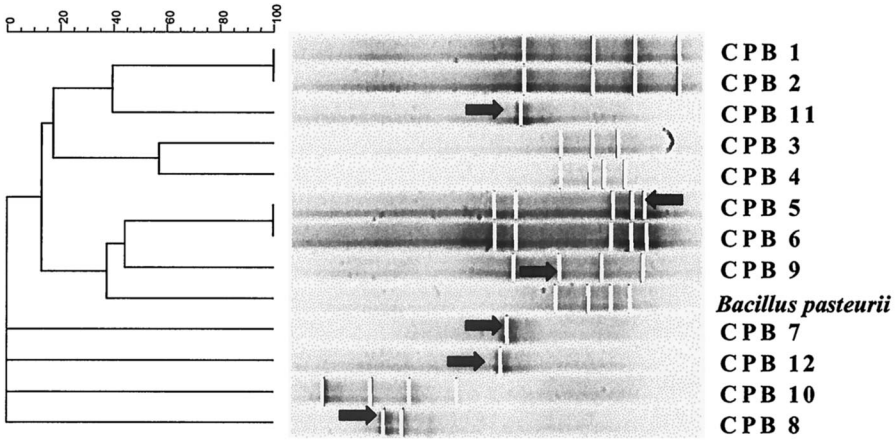

FIG. 4. DGGE separation of selectively amplified urease PCR products from the different isolates, with *B. pasteurii* as a positive control. The tree was constructed by calculating the Dice coefficient and clustering with an unweighted pair group with mathematical average algorithm. The white vertical lines represent bands, and individual bands indicated by arrows were excised and sequenced, as described in the text.

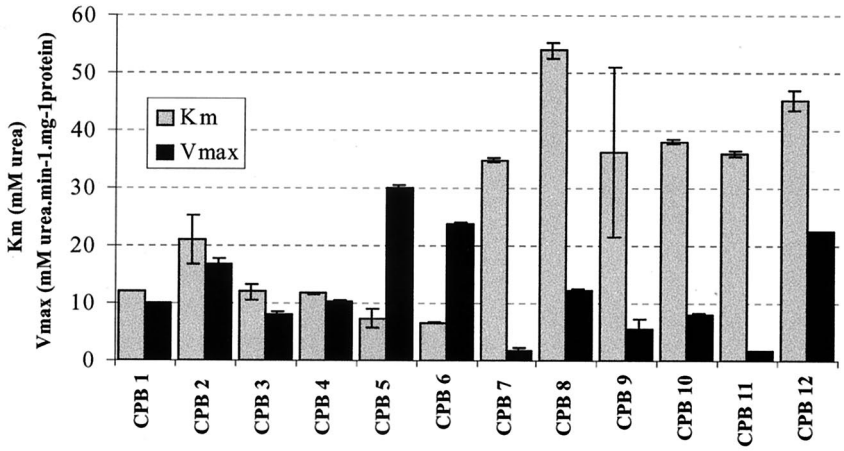

FIG. 5. Michaelis-Menten kinetic values (K_m and V_{max}) determined with crude enzyme extracts from the various ureolytic calcium-precipitating isolates. The error bars indicate standard deviations.

resulting in removal of 99% of the calcium. Interestingly, during adaptation of this reactor community, the bacterial community changed, but urease activity was apparently dominated by only two ureases (15).

Precipitation within microbial colonies on agar presents a unique opportunity to study MCP within a specific localized microenvironment created by the microorganisms (Fig. 1). In previous studies workers have used XRD data to suggest that species-specific microbial precipitation occurs (19, 31), but other workers contend that species-specific differences are due primarily to environmental rather than microbial factors (20). Although morphological differences in crystallization were evident (Fig. 2), XRD analysis showed that in all cases rhombohedral calcite was the primary component, with vaterite detected only in some cases. The latter finding is interesting, as vaterite is metastable at the normal temperature and atmospheric pressure, and it has been suggested that the metastable polymorphs form initially and subsequently convert to a stable polymorph (e.g., calcite) (39). Enzymatic precipitation experiments performed with liquid solutions of urea and $CaCl_2$ at room temperature revealed that the sequence of precipitation is as follows: first amorphous $CaCO_3$, then vaterite, and finally calcite (35). Although calcite is commonly precipitated during ureolytic carbonate precipitation (37), microbes precipitate other polymorphs, such as aragonite (19, 31). The fact that all the samples produced very similar XRD results, while clear morphological differences were evident, suggests that the differences were a result of variations in crystal growth rates along different planes of the crystal structure. This could have been a result of the colony growth rate and/or actual urease activity, which thus influenced the rate of supply of chemical species required for precipitation (35). Alternatively, crystal growth can be inhibited or altered by the adsorption of proteins, organic matter, or inorganic components to specific crystallographic planes of the growing crystal (19, 30, 34).

Initially, we hypothesized that the differences in crystal morphology arose because the bacteria belonged to different genera. Thus, it was surprising that for such a widespread function as urease the isolates obtained were all so closely related to the *B. sphaericus* group. Several ureolytic $CaCO_3$-precipitating

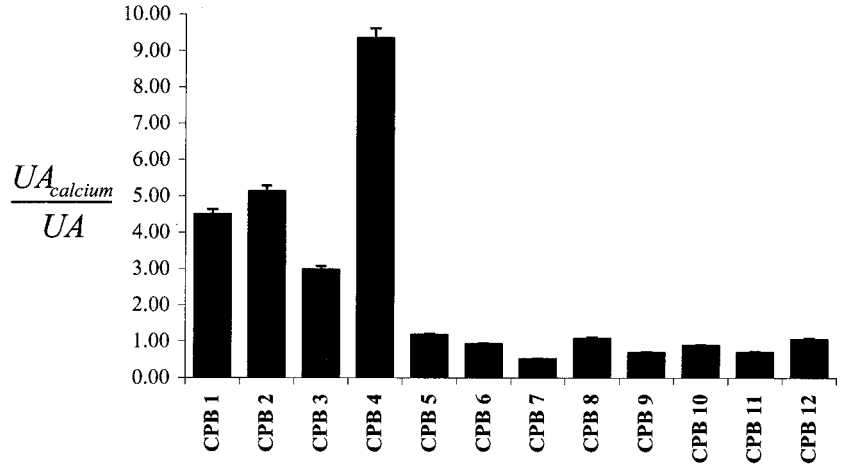

FIG. 6. Effect of calcium ions (30 mM) on the specific urease activities (100 mM urea assay) of the various isolates, expressed as the urease activity with calcium ($UA_{calcium}$) divided by the urease activity without calcium present (UA). The error bars indicate standard deviations.

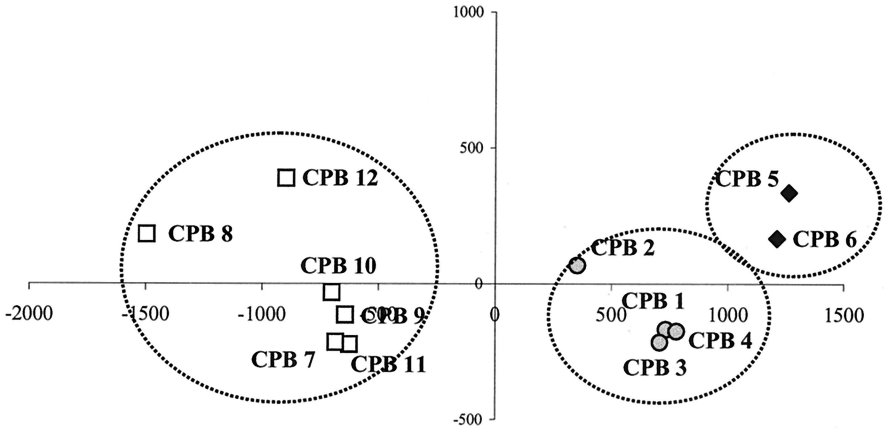

FIG. 7. PCA incorporating biochemical and molecular urease data and revealing at least three major clusters.

species have been characterized previously, including *B. pasteurii* (12, 37), *Pseudomonas* spp. and *Variovorax* spp. (13), and *Leuconostoc mesenteroides* (12). We therefore emphasize that the isolation and identification results presented here do not necessarily represent a unique group of calcium-precipitating bacteria but rather represent organisms that proliferate and express the urease gene under the cultivation conditions used. However, the close relationship of the various isolates obtained in this study within the *B. sphaericus* group is remarkable. To some extent, the predominance of a specific phylogenetic group can be attributed to the environments from which the isolates were obtained. Both the soils and the concrete surface represent dry conditions in which spore-forming organisms, such as *Bacillus* species, proliferate. In this regard Felske et al. (10), for instance, showed with fluorescent in situ hybridization that at least 40% of all bacteria in a Dutch soil belonged to *Bacillus* species and some other low-G+C-content organisms. The isolation and cultivation conditions could also have had a selective influence; nutrient broth with urea added is a preferred growth medium of ureolytic *Bacillus* species (12, 37). Confirming this, when nonculturing methods are used, urease biotechnology reactors are dominated by a variety of bacterial species (15). Thus, the significance of the *B. sphaericus* group is unknown, but the observation that marked differences in crystal morphology occurred among closely related species suggests that further research is needed to determine how bacteria precipitate $CaCO_3$ in order to optimize biotechnological applications of this process.

A new approach to study the diversity of functional genes is analysis of PCR products of these genes with DGGE (4, 32). To our knowledge, this is the first study in which DGGE was used to examine the diversity of a urease gene fragment. The first noticeable result of the urease DGGE analysis is the apparent presence of isozymes. Although the presence of urease isoforms in a single organism has been described previously (7), the notion of multiple isozymes has been largely rejected (25). DGGE examination of PCR products amplified with degenerated primers often reveals more than one band from a single unique starting template (21). The generation of multiple bands was, however, not entirely consistent, since not all CPB DNA templates resulted in multiple bands (Fig. 4). As a consequence, in some of the CPB strains isolated, the possibility that there are different isozymes cannot be excluded. DGGE also revealed distinct differences as well as evident similarities between isolates, which were highlighted by the cluster analysis (Fig. 4). Interestingly, some correlation between the clustering results and the crystal groups could be detected. For example, the 100% similarity between CPB 1 and CPB 2 and the 100% similarity between CPB 5 and CPB 6 coincide with the corresponding distinct and almost identical crystallization patterns (Fig. 2). On the other hand, *B. pasteurii* clustered with CPB 5, CPB 6, and CPB 9, in contrast to the phylogenetic clustering (Fig. 3). These results confirm previous reports that there is a definite degree of divergence in the genetic make-up of microbial ureases (25, 26). DGGE makes it possible to reveal this urease diversity, since this technique reveals a 1-bp difference between two sequences (11). This DGGE approach, applied to total DNA extracted from various environmental habitats, could be especially useful for further investigation of the diversity of urease genes in microbial communities without prior cultivation of the urease-positive organisms.

The results reported here showed that urease activity was present in all the isolates and that the urease enzymes were not extracellular in any of the isolates, which was consistent with most of the previously described data concerning this point (7, 25, 37). K_m values for urease enzymes ranging from 0.1 to 100 mM urea have been reported for bacteria (24), suggesting that the values obtained for CPB 7 to CPB 12 (35 to 55 mM) reflect rather low substrate affinities. On the other hand, the V_{max} values for most isolates were rather high. Stocks-Fisher et al. (37) reported a V_{max} value for *B. pasteurii* urease of 1.72 to 3.55 $mM \cdot min^{-1} \cdot mg\ of\ protein^{-1}$ (depending on the pH). The standard reported values range from 1 to 5.5 $mM \cdot min^{-1} \cdot mg\ of\ protein^{-1}$ for purified microbial enzymes, while *Ureoplasma ureolyticum* was shown to have values between 33 and 180 $mM \cdot min^{-1} \cdot mg\ of\ protein^{-1}$ (25). Crude enzyme extracts should be used comparatively rather than as preparations that are reflective of the actual urease activity of an organism, as the actual urease activity is significantly affected by transmembrane transport of urea (via urea permease enzymes), ammonia, and protons. Nonetheless, the activity results in Fig. 5 do explain to some extent the differences seen in crystallization. Isolates CPB 1 to CPB 6 all exhibited moderate to high sub-

strate affinities and high specific rates, which resulted in rapid crystallization of $CaCO_3$ aggregates that were crystalline in appearance and had a clear to light-brown color. This was especially the case for isolates CPB 5 and CPB 6. Isolates CPB 7 to CPB 12, representing the initial classes 5 and 6, displayed low substrate affinities and low specific rates (with the exception of isolate CPB 12, which displayed a rather high specific rate). This could explain the slower crystal formation, which allowed more colony growth, and thus the interference by the sorption of organic matter in the crystal structure. The latter would have caused both the less crystalline appearance of the aggregates and the darker color.

The presence of calcium modulated urease activity. Southam (36) suggested that surface-associated mineralization could result in limitations of nutrient transport and eventual disruption of the proton motive force, which suggested that precipitation resulting from urea hydrolysis might be detrimental to bacterial cells and thus to further urease activity. Figure 6 shows that for most of the isolates no difference was detected between urease activity in the presence of calcium and urease activity in the absence of calcium. However, isolates CPB 1 to CPB 4 exhibited remarkable increases in urease activity in the presence of soluble calcium. This coincides with characteristic similar macrocrystallization by these isolates (Fig. 2) and strengthens the conclusion described above that high urease affinities and high specific rates were the basis of the differences in macrocrystallization. To our knowledge, calcium ions have not previously been associated with increased urease activity. While Ca^{2+} could theoretically facilitate better transmembrane transport or improve intracellular signaling processes, it should be expected that these processes occur in all related organisms, such as the case described here. An alternative possibility is a detoxification response of the bacteria to high calcium concentrations (17). Active calcium metabolism requires energy (ATP) (23), and several microorganisms (e.g., *B. pasteurii*) have previously been shown to produce ATP through urea hydrolysis (25). The fact that some strains displayed such a pronounced effect warrants further research on the possibilities of an ATP-driven calcification process.

In conclusion, in this paper we clearly show that strain-specific precipitation occurs during ureolytic microbial $CaCO_3$ precipitation in a closely related group of bacteria. The differences in precipitation could largely be ascribed to diversity in the urease enzymes of the various isolates, coupled to the pronounced effect of calcium on urease activity in some strains.

ACKNOWLEDGMENTS

This research was sponsored in part by an equipment grant from the Flemish Fund for Scientific Research (FWO-Vlaanderen).

We thank Sabine Verryn for performing the XRD analysis and phase identification, R. Hausinger for providing comments on the urease molecular results, and Vanessa Vermeirsen, Hanne Lievens, and Sofie Dobelaere for critically reading the manuscript.

REFERENCES

1. **Altschul, S. F., T. L. Madden, A. A. Schaffer, J. Zhang, Z. Zhang, W. Miller, and D. J. Lipman.** 1997. Gapped BLAST and PSI-BLAST: a new generation of protein database search programs. Nucleic Acids Res. **25:**3389–3402.
2. **Anderson, S., V. D. Appanna, J. Huang, and T. Viswanatha.** 1992. A novel role for calcite in calcium homeostasis. FEBS Lett. **308:**94–96.
3. **Boon, N., J. Goris, P. De Vos, W. Verstraete, and E. M. Top.** 2000. Bioaugmentation of activated sludge by an indigenous 3-chloroaniline-degrading *Comamonas testosteroni* strain, I2gfp. Appl. Environ. Microbiol. **66:**2906–2913.
4. **Boon, N., J. Goris, P. De Vos, W. Verstraete, and E. M. Top.** 2001. Genetic diversity among 3-chloroaniline- and aniline-degrading strains of the *Comamonadaceae*. Appl. Environ. Microbiol. **67:**1107–1115.
5. **Boquet, E., A. Boronat, and A. Ramos-Cormenzana.** 1973. Production of calcite (calcium carbonate) crystals by soil bacteria is a general phenomenon. Nature (London) **246:**527–529.
6. **Bradford, M. M.** 1976. A rapid and sensitive method for the quantitation of microgram quantities of protein utilizing the principle of protein-dye binding. Anal. Biochem. **72:**248–254.
7. **Burne, R. A., and Y. Y. Chen.** 2000. Bacterial ureases in infectious diseases. Microbes Infect. **2:**533–542.
8. **Castanier, S., G. Le Métayer-Levrel, and J. P. Perthuisot.** 1999. Ca-carbonates precipitation and limestone genesis—the microbiologist point of view. Sediment. Geol. **126:**9–23.
9. **Douglas, S., and T. J. Beveridge.** 1998. Mineral formation by bacteria in natural microbial communities. FEMS Microbiol. Ecol. **26:**79–88.
10. **Felske, A., A. D. L. Akkermans, and W. M. De Vos.** 1998. In situ detection of an uncultured predominant *Bacillus* in Dutch grassland soils. Appl. Environ. Microbiol. **64:**4588–4590.
11. **Felske, A., A. Wolterink, R. Van Lis, W. M. De Vos, and A. D. L. Akkermans.** 1999. Searching for predominant soil bacteria: 16S rDNA cloning versus strain cultivation. FEMS Microbiol. Ecol. **30:**137–145.
12. **Ferris, F. G., and L. G. Stehmeier.** January 1993. Bacteriogenic mineral plugging. U.S. patent 5,143,155
13. **Fujita, Y., F. G. Ferris, R. D. Lawson, F. S. Colwell, and R. W. Smith.** 2000. Calcium carbonate precipitation by ureolytic subsurface bacteria. Geomicrobiol. J. **17:**305–318.
14. **Greenberg, A. E., L. S. Clesceri, and A. D. Eaton (ed.).** 1992. Standard methods for the examination of water and wastewater, 18th ed. American Public Health Association, Washington, D.C.
15. **Hammes, F., N. Boon, G. Clement, J. de Villiers, S. D. Siciliano, and W. Verstraete.** Molecular, biochemical and ecological characterisation of a biocatalytic calcification reactor. Appl. Microbiol. Biotechnol., in press.
16. **Hammes, F., A. Seka, S. De Knijf, and W. Verstraete.** 2003. A novel approach to calcium removal from calcium-rich industrial wastewater. Water Res. **37:**699–704.
17. **Hammes, F., and W. Verstraete.** 2002. Key roles of pH and calcium metabolism in microbial carbonate precipitation. Re. Environ. Sci. Bio/Technol. **1:**3–7.
18. **Jukes, T. H., and C. R. Cantor.** 1969. Evolution of protein molecules, p. 21–132. *In* H. N. Munro (ed.), Mammalian protein metabolism. Academic Press, Inc., New York, N.Y.
19. **Kawaguchi, T., and A. W. Decho.** 2002. A laboratory investigation of cyanobacterial extracellular polymeric secretions (EPS) in influencing $CaCO_3$ polymorphism. J. Cryst. Growth **240:**230–235.
20. **Knorre, H., and W. Krumbein.** 2000. Bacterial calcification, p. 25–31. *In* R. E. Riding and S. M. Awramik (ed.), Microbial sediments. Springer-Verlag, Berlin, Germany.
21. **Kowalchuk, G., J. Stephen, W. De Boer, J. Prosser, T. Embley, and J. Woldendorp.** 1997. Analysis of ammonia-oxidizing bacteria of the beta subdivision of the class *Proteobacteria* in coastal sand dunes by denaturing gradient gel electrophoresis and sequencing of PCR-amplified 16S ribosomal DNA fragments. Appl. Environ. Microbiol. **63:**1489–1497.
22. **Maidak, B. L., J. R., Cole, T. G. Lilburn, C. T. Parker, Jr., P. R. Saxman, R. J. Farris, G. M. Garrity, G. J. Olsen, T. M. Schmidt, and J. M. Tiedje.** 2001. The RDP-II (Ribosomal Database Project). Nucleic Acids Res. **29:**173–174.
23. **McConnaughey, T. A., and F. F. Whelan.** 1997. Calcification generates protons for nutrient and bicarbonate uptake. Earth Sci. Rev. **42:**95–117.
24. **McKay, D. S., E. K. Gibson, Jr., K. Thomas-Keprta, H. Vali, C. S. Romanek, S. J. Clemett, X. D. F. Chillier, C. R. Maechling, and R. N. Zare.** 1996. Search for past life on Mars: possible relic biogenic activity in Martian meteorite ALH84001. Science **273:**924–930.
25. **Mobley, H. L. T., and R. P. Hausinger.** 1989. Microbial ureases: significance, regulation and molecular characterization. Microbiol. Rev. **53:**85–108.
26. **Mobley, H. L. T., M. D. Island, and R. P. Hausinger.** 1995. Molecular biology of microbial ureases. Microbiol. Rev. **59:**451–480.
27. **Muyzer, G., E. C. De Waal, and A. Uitterlinden.** 1993. Profiling of complex microbial populations using denaturing gradient gel electrophoresis analysis of polymerase chain reaction-amplified genes coding for 16S rRNA. Appl. Environ. Microbiol. **59:**695–700.
28. **Peckman, J., J. Paul, and V. Thiel.** 1999. Bacterially mediated formation of diagenetic aragonite and native sulphur in Zechstein carbonates (Upper Permian, central Germany). Sediment. Geol. **126:**205–222.
29. **Reed, K. E.** 2001. Restriction enzyme mapping of bacterial urease genes: using degenerate primers to expand experimental outcomes. Biochem. Mol. Biol. Edu. **29:**239–244.
30. **Rivadeneyra, M. A., G. Delgado, A. Ramos-Cormenzana, and R. Delgado.** 1998. Biomineralisation of carbonates by *Halomonas eurihalina* in solid and liquid media with different salinities: crystal formation sequence. Res. Microbiol. **149:**277–287.
31. **Rivadeneyra, M. A., G. Delgado, M. Soriano, A. Ramos-Cormenzana, and R.**

Delgado. 2000. Precipitation of carbonates by *Nesterenkonia halobia* in liquid media. Chemosphere **41:**617–624.
32. **Rosado, A. S., G. F. Duarte, L. Seldin, and J. D. Van Elsas.** 1998. Genetic diversity of *nifH* gene sequences in *Paenibacillus azotofixans* strains and soil samples analyzed by denaturating gradient gel electrophoresis of PCR-amplified gene fragments. Appl. Environ. Microbiol. **64:**2770–2779.
33. **Saitou, N., and M. Nei.** 1987. The neighbor-joining method: a new method for reconstructing phylogenetic trees. Mol. Biol. Evol. **4:**406–425.
34. **Schultze-Lam, S., D. Fortin, B. S. Davis, and T. J. Beveridge.** 1996. Mineralisation of bacterial surfaces. Chem. Geol. **132:**171–181.
35. **Sondi, I., and E. Matijevic.** 2001. Homogeneous precipitation of calcium carbonates by enzyme catalyzed reaction. J. Colloid Interface Sci. **238:**208–214.
36. **Southam, G.** 2000. Bacterial surface-mediated mineral formation, p. 257–276. *In* D. R. Lovley (ed.), Environmental microbe-metal interactions. ASM Press, Washington D.C.
37. **Stocks-Fisher, S., J. K. Galinat, and S. S. Bang.** 1999. Microbiological precipitation of $CaCO_3$. Soil Biol. Biochem. **31:**1563–1571.
38. **Trewin, N. H., and A. H. Knoll.** 1999. Preservation of Devonian chemotrophic filamentous bacteria in calcite veins. Palaios **14:**288–294.
39. **Vecht, A., and T. G. Ireland.** 2000. The role of vaterite and aragonite in the formation of pseudo-biogenic carbonate structures: implications for Martian exobiology. Geochim. Cosmochim. Acta **66:**2719–2725.
40. **Westfall, F.** 1999. The nature of fossil bacteria: a guide to the search for extraterrestrial life. J. Geophys. Res. E Planets **104:**16437–16451.